

## Supporting Information

# Semi-Rational Hinge Engineering: Modulating the Conformational Transformation of Glutamate Dehydrogenase for Enhanced Reductive Amination Activity towards Non-Natural Substrates

### Authors and Affiliation:

Xinjian Yin<sup>†</sup>, Yayun Liu, Lijun Meng, Haisheng Zhou, Jianping Wu,\* and Lirong Yang,\*

*Institute of Bioengineering, College of Chemical and Biological Engineering, Zhejiang University, Hangzhou, 310027, China*

### Corresponding authors:

\*E-mail: wjp@zju.edu.cn

\*E-mail: lryang@zju.edu.cn

<sup>†</sup> Present address: *School of Marine Sciences, Sun Yat-sen University, Guangzhou, 510006, China*

## Contents List

**Figure S1.** PPO catalytic activity of the positive mutants acquired in error-prone PCR based directed evolution

**Figure S2.** Back mutation analysis of multi-residues substituted mutants acquired in error-prone PCR based directed evolution

**Figure S3.** Back mutation analysis of multi-residues substituted mutants from library C and D

**Figure S4.** Distance-K137/A291 difference between the “open” and “closed” subunits of *PpGluDH* protein

**Figure S5.** Pre-column derivatization HPLC analysis of *ee* value of the formed L-Phosphinothricin

**Figure S6.** Pre-column derivatization HPLC analysis of *ee* value of the formed L-Homophenylalanine

**Figure S7.** Pre-column derivatization HPLC analysis of *ee* value of the formed L-2-aminobutyric acid

➤ **Hinge engineering of active-site tailored GluDHs- supplementary data:**

**Table S1.** The information of active-site tailored GluDHs

**Figure S8.** Amino acid sequence alignment of GluDHs

**Figure S9.** The location of the targeted residue in the three-dimensional structure of GluDHs

**Figure S10.** The screening result of Mutagenesis libraries.

**Figure S11.** Schematic of saturation mutagenesis libraries construction using the One-step Cloning Kit

➤ **The information of the coenzyme regeneration enzymes used in this study**

➤ **The primers used in this study**

**Table S2.** The primers for error-prone PCR

**Table S3.** The primers for saturation mutagenesis libraries construction

**Table S4.** The primers for back mutation analysis

**Figure S12.** SDS-PAGE analysis of purified *Pp*GluDH wild type (WT) and mutants.

**Figure S13.** Plots for the determination of  $\text{NH}_4^+$  and NADPH saturation values

**Figure S14.** Michaelis-Menten plots for the kinetics of the hinge-engineered mutants with PPO

**Figure S15.** Mass spectrum (MS) of the synthesized substrate 2-oxo-4-[(hydroxy)(methyl)phosphinyl]butyric acid (PPO)

**Figure S16.** NMR spectra of the synthesized substrate 2-oxo-4-[(hydroxy)(methyl)phosphinyl]butyric acid (PPO)

**Figure S17.** Mass spectrum (MS) of the synthesized substrate 2-oxoheptanoic acid

**Figure S18.** NMR spectra of the synthesized substrate 2-oxoheptanoic acid

**Figure S19.** Mass spectrum (MS) of the synthesized substrate 2-oxooctanoic acid

**Figure S20.** NMR spectra of the synthesized substrate 2-oxooctanoic acid

**Figure S21.** Mass spectrum (MS) of the synthesized substrate 2-oxononanoic acid

**Figure S22.** NMR spectra of the synthesized substrate 2-oxononanoic acid

➤ **Purification process of the formed L-amino acids**

**Figure S23.** Mass spectrum (MS) of the purified L-phosphinothricin

**Figure S24.** NMR spectra of the purified L-phosphinothricin

**Figure S25.** Mass spectrum (MS) of the purified L-2-aminobutyric acid

**Figure S26.** NMR spectra of the purified L-2-aminobutyric acid

**Figure S27.** Mass spectrum (MS) of the purified L-homophenylalanine

**Figure S28.** NMR spectrum of the purified L-homophenylalanine

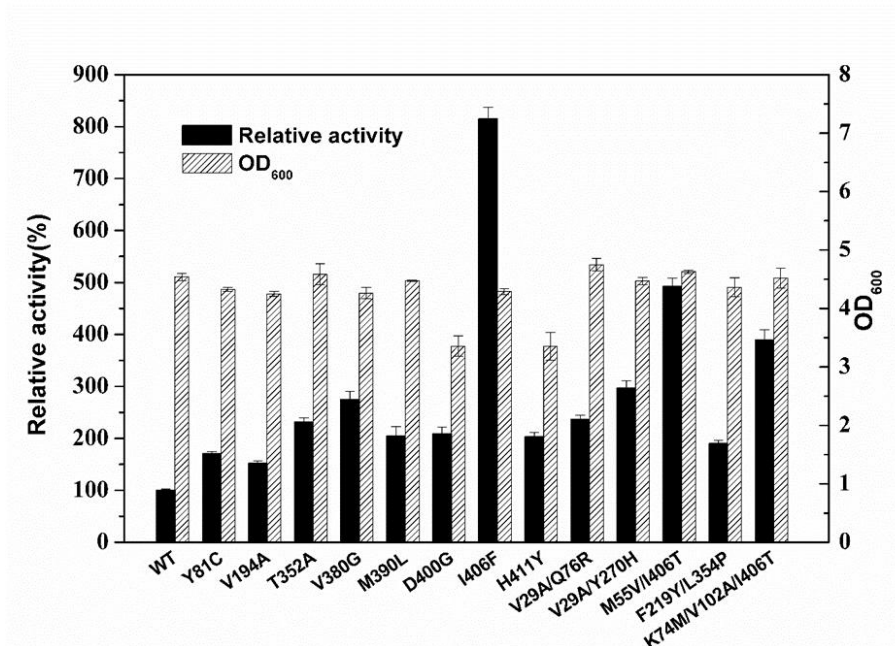


**Figure S1.** PPO catalytic activity of the positive mutants acquired in error-prone PCR based directed evolution. Relative activity is expressed as a percentage of wild type *Pp*GluDH specific volume activity (0.11 U/mL) under the experimental conditions.

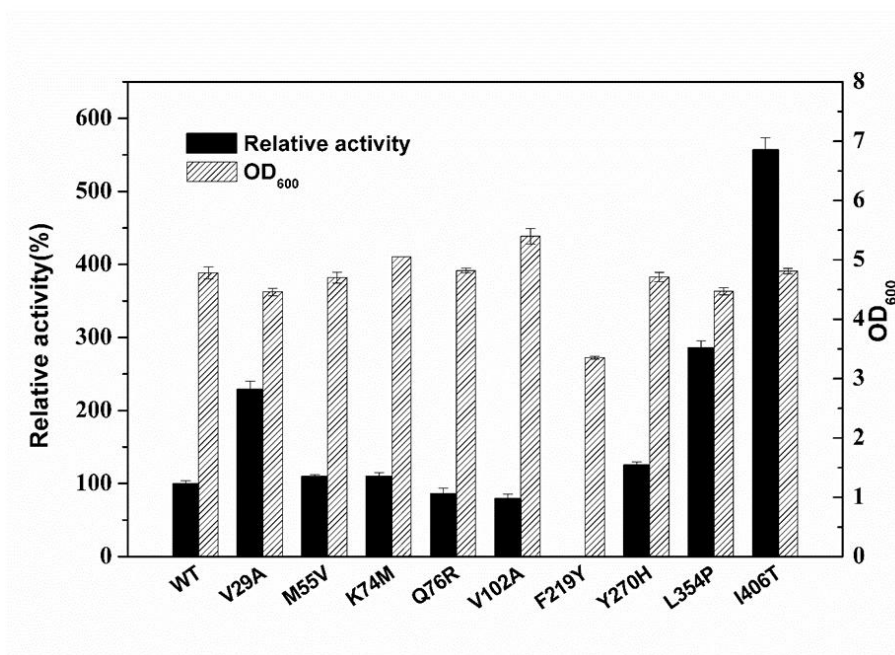


**Figure S2.** Back mutation analysis of multi-residues substituted mutants acquired in error-prone PCR based directed evolution. Relative activity is expressed as the percentage of wild type *Pp*GluDH specific volume activity (0.11 U/mL) in the experimental conditions.

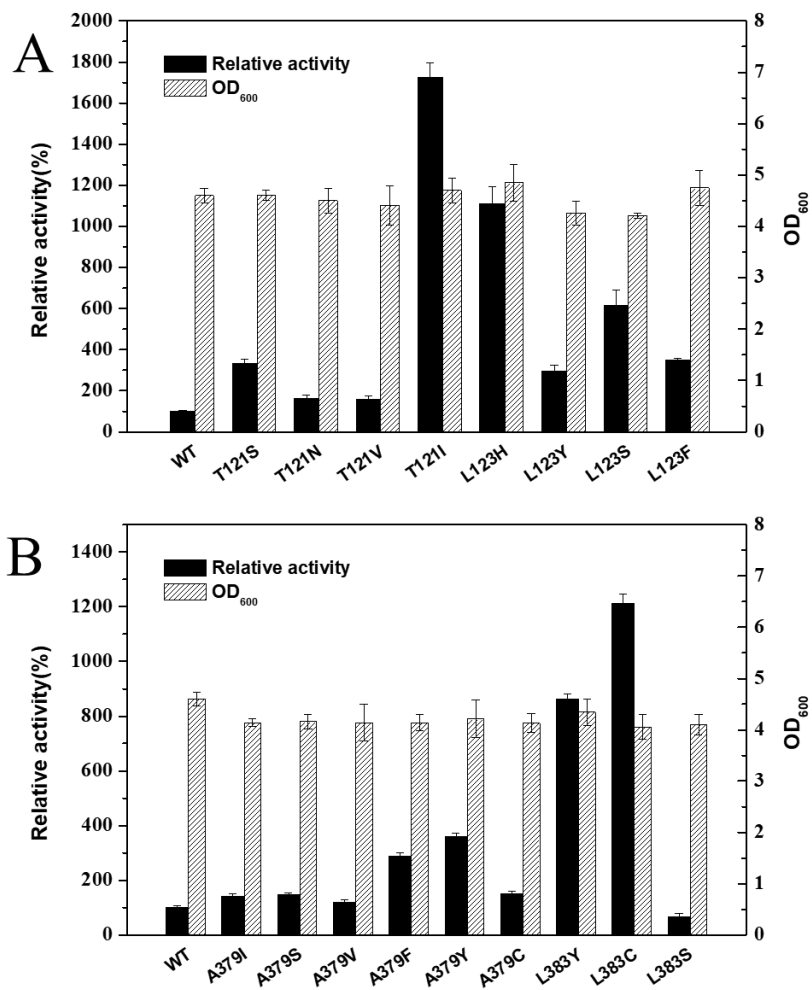


**Figure S3.** Back mutation analysis of multi-residues substituted mutants from library C and D. (A) library C; (B) library D. Relative activity is expressed as the percentage of wild type *PpGluDH* specific volume activity (0.11 U/mL) in the experimental conditions.

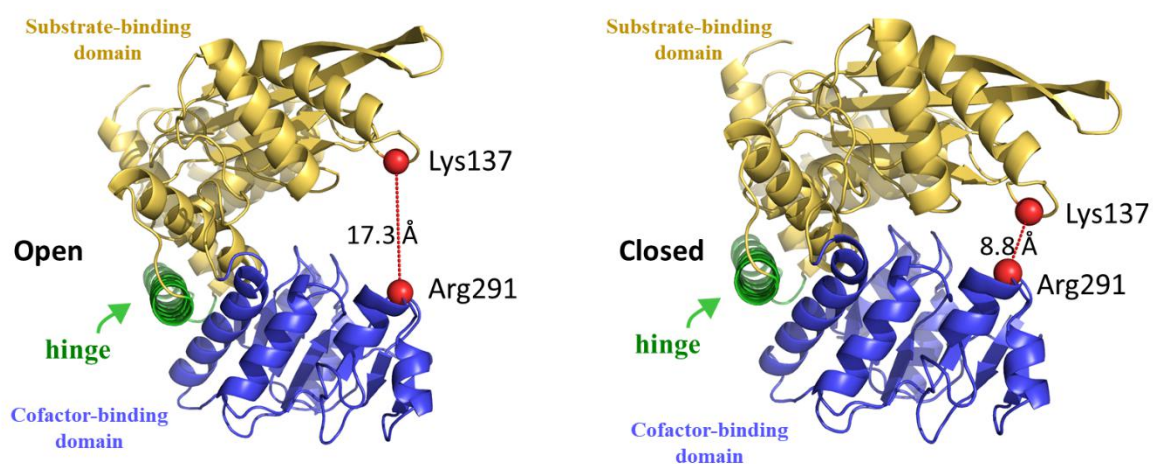


**Figure S4.** Distance-K137/A291 difference between the “open” and “closed” subunits of *PpGluDH* protein. The substrate-binding domain is represented in yellow, the cofactor-binding domain is represented in blue and the hinge is represented in green.

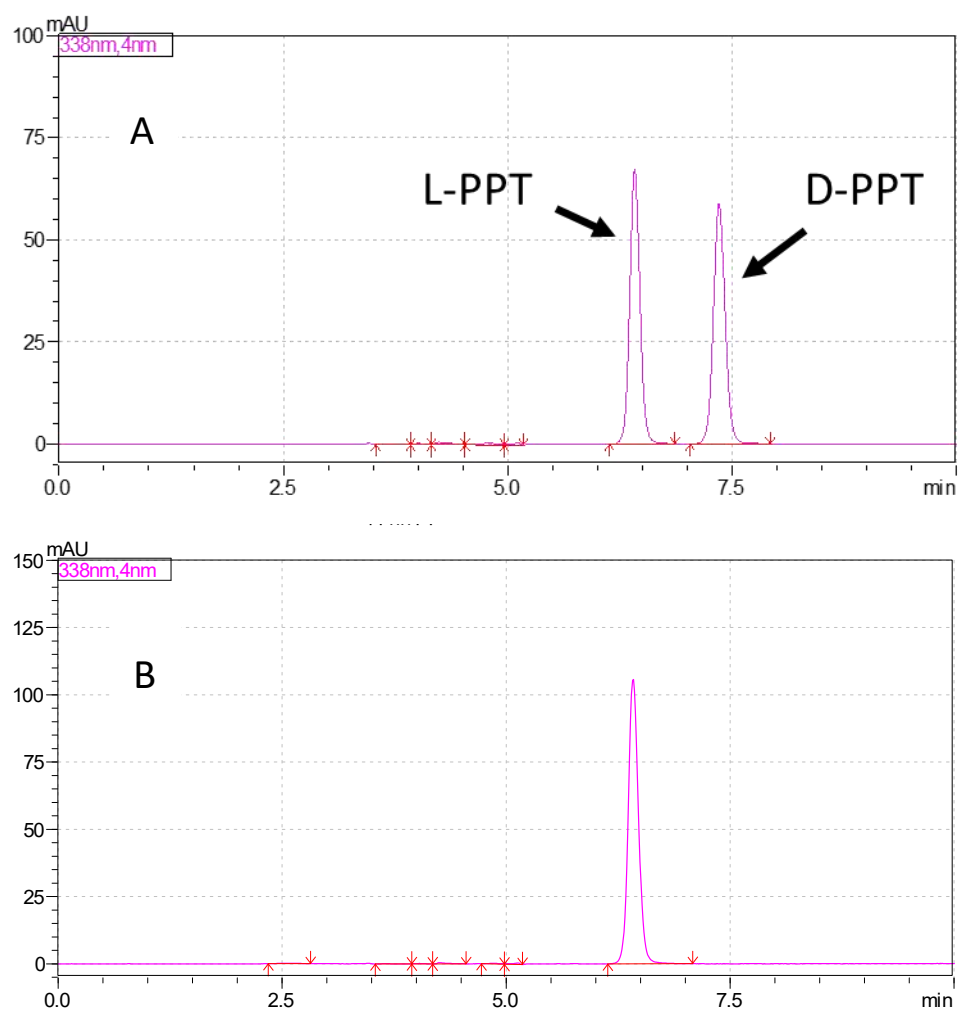


**Figure S5.** Pre-column derivatization HPLC analysis of *ee* value of the formed L-phosphinothricin. (A) HPLC spectrum of the racemic D,L-phosphinothricin (D,L-PPT) standard sample. (B) HPLC spectrum of the formed product in final reaction mixture of the batch reaction.

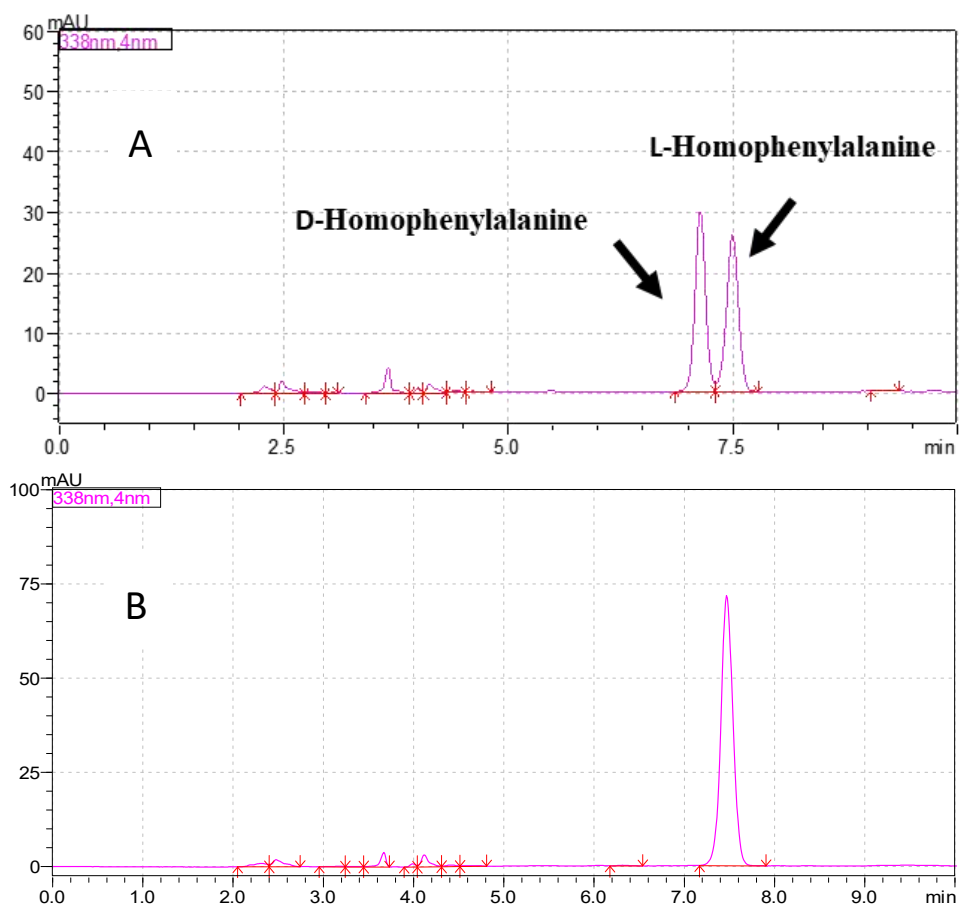


**Figure S6.** Pre-column derivatization HPLC analysis of *ee* value of the formed L-homophenylalanine. (A) HPLC spectrum of the racemic D,L-homophenylalanine standard sample. (B) HPLC spectrum of the formed L-homophenylalanine in final reaction mixture of the batch reaction.

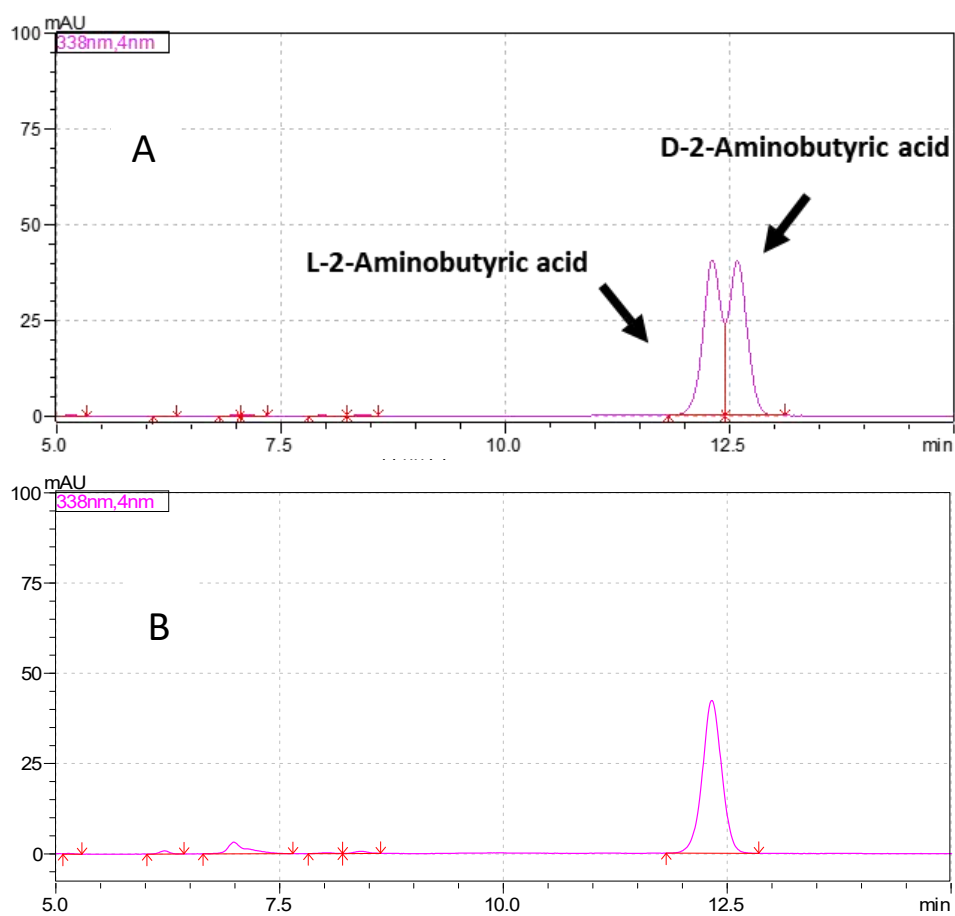


**Figure S7.** Pre-column derivatization HPLC analysis of *ee* value of the formed L-2-aminobutyric acid. (A) HPLC spectrum of the racemic D,L-2-aminobutyric acid standard sample. (B) HPLC spectrum of the formed L-2-aminobutyric acid in final reaction mixture of the batch reaction.



## Hinge engineering of active-site tailored GluDHs- supplementary data

### 1) The information of selected active-site tailored GluDHs

In addition to *Pp*GluDH-A167G, we also performed hinge engineering to other two active-site tailored GluDHs, including *Ec*GluDH-A166G and *Cs*GluDH-A164G. The detail information of these two active-site tailored GluDHs were listed in Table S1.<sup>[1]</sup>

**Table S1.** The information of active-site tailored GluDHs

GluDHs	Source	Coenzyme specificity	Sequence Homology (%) <sup>a)</sup>	Active-site mutation	Activity (U/mL) <sup>b)</sup>
<i>Pp</i> GluDH-A167G	<i>Pseudomonas putida</i>	NADP(H)	100	A167G	14.9
<i>Ec</i> GluDH-A166G	<i>Escherichia coli</i>	NADP(H)	64.8	A166G	26.05
<i>Cs</i> GluDH-A164G	<i>Clostridium symbiosum</i>	NAD(H)	53.4	A164G	2.61

a) The sequence homology was measured with the amino acid sequence of *Pp*GluDH as reference.

b) The specific volume activity of the active-site tailored GluDHs toward PPO.

### 2) Saturation mutagenesis libraries design

The residues of *Ec*GluDH-A166G and *Cs*GluDH-A164G corresponding to *Pp*GluDH's Ile406 were targeted by multiple sequence alignment (**Figure S8**). As shown in homology model of *Ec*GluDH and *Cs*GluDH, the selected residues (Ile405 of *Ec*GluDH and Val406 of *Cs*GluDH) also located on the hinge structure (**Figure S9**). NNK codon degeneracy were used for the construction of saturation mutagenesis. In general, two focused libraries were constructed, namely, *Ec*GluDH-A166G/I405X and *Cs*GluDH-A164G/V406X.

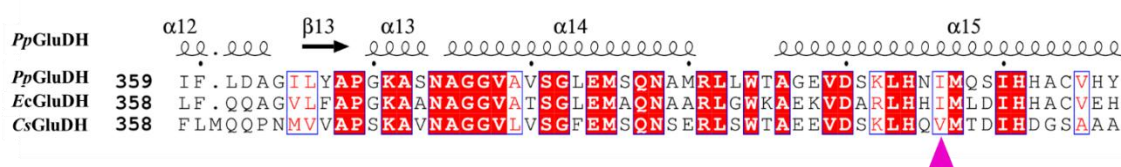


**Figure S8.** Amino acid sequence alignment of GluDHs. Alignment was performed using the T-Coffee server (<http://tcoffee.vital-it.ch/apps/tcoffee/do:regular>) and displayed using Esprit (<http://esprit.ibcp.fr>). Ile406 (*Pp*GluDH numbering) are marked with purple triangles.

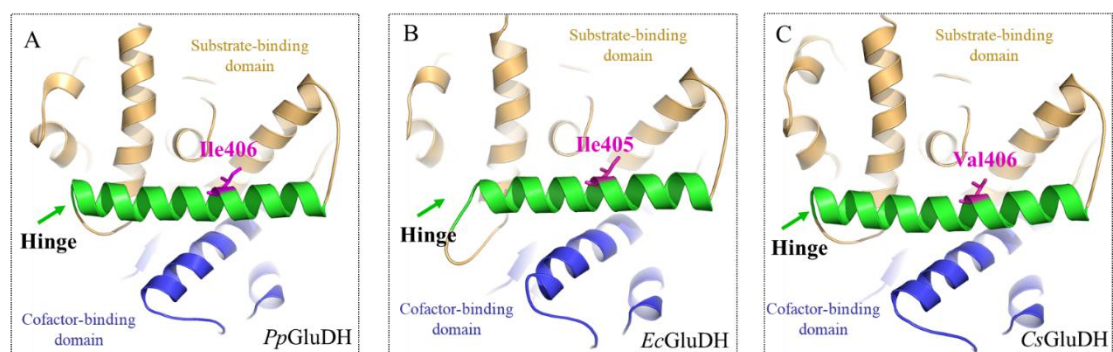


**Figure S9.** The location of the targeted residue in the three-dimensional structure of GluDHs. (A) The homology model of *PpGluDH*; (B) The three-dimensional structure of *EcGluDH* (PDB ID: 3SBO); (C) The three-dimensional structure of *CsGluDH* (PDB ID: 1BGV). The substrate-binding domain is represented in orange, the cofactor-binding domain is represented in blue and the hinge is represented in green. The Ile406 (*PpGluDH* numbering) is represented as stick model with purple.

### 3) Mutagenesis libraries screening

High-throughput primary screening and HPLC rescreening were carried out with PPO as the substrate. As shown in Figure S10, positive mutants with significantly improved PPO-oriented activity were identified from the two libraries, suggesting the general applicability of the hinge engineering for enhancing reductive amination activity of GluDHs.

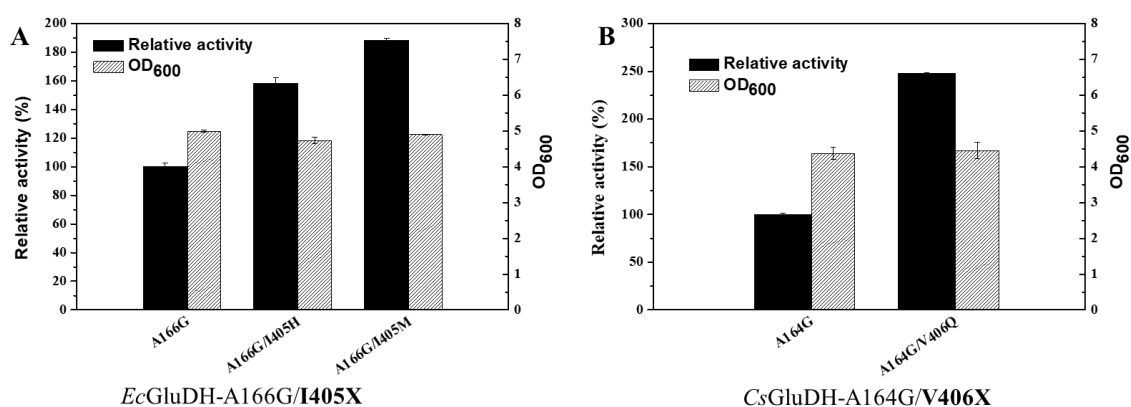


**Figure S10.** The screening result of Mutagenesis libraries. (A) Library *EcGluDH*-A166G/I405X; Relative activity is expressed as the percentage of *EcGluDH*-A166G specific volume activity (26.05 U/mL) in the experimental conditions; (B) Library *CsGluDH*-A164G/V406X. Relative activity is expressed as the percentage of *CsGluDH*-A164G specific volume activity (2.61 U/mL) in the experimental conditions.

## References :

[1] Yin, X J.; Liu, Y Y.; Meng, L J.; Zhou, H S.; Wu, J.; Yang, L R., *Advanced Synthesis & Catalysis* 2019, 361 (4), 803-812.

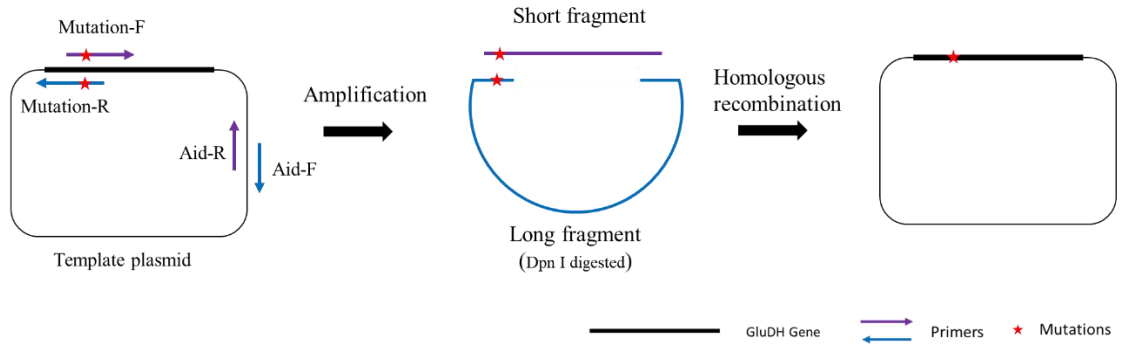


**Figure S11.** Schematic of saturation mutagenesis libraries construction using the One-step Cloning Kit

## The information of the coenzyme regeneration enzymes used in this study.

1) Amino acid sequence of the glucose dehydrogenase<sup>a)</sup> used in this study:

MYPDLKKGKVVAITGAASGLGKAMAIRFGKEQAKVVINYYSNKQDPNEVKEE  
VIKAGGEAVVVQGDVTKEEDVKNIVQTAIKEFGTLDIMINNAGLENPVPSHEM  
PLKDWDKVIQTNLTGAFLGSREAIKYFVENDIKGNVINMSSVHEVIPWPLFVH  
YAASKGGIKLMTRTLALEYAPKGRVNNIGPGAINTPINAEKFADPKQKADVES  
MIPMGYIGEPEEIAAVAAWLASKEASYVTGITLFADGGMTLYPSFQAGR\*

<sup>a)</sup>This glucose dehydrogenase was cloned from *Bacillus subtilis* 168, and the E170 (glutamate) and Q252 (glutamine) were mutated to R(arginine) and L(leucine) respectively for the improvement of thermostability.<sup>[1]</sup>

2) Amino acid sequence of the alcohol dehydrogenase<sup>b)</sup> used in this study:

MKGFAMLSIGKVGWIEKEKPAPGPFDAIVRPLAVAPCTSDIHTVFEGAIGERHN  
MILGHEAVGEVVEVGSEVKDFKPGDRVVVPAITPDWRTSEVQRGYHQHSGG  
MLAGWKFSNVKDGVFGEFFHVNDADMNLAHLPKEIPLEAAVMIPDMMTTGF  
HGAELADIELGATVAVLGIGPVGLMAVAGAKLRGAGRIIIVGSRPVCVDAKY  
YGATDIVNYKDGPIESQIMNLTEGKGVDAIIAGGNADIMATAVKIVKPGGTIA  
NVNYFGEGEVLPVPRLEWGCGMAHKTIKGGLCPGGRLRMERLIDLVFYKRV  
DPSKLVTHVFRGFDNIEKAFMLMKDKPKDLIKPVVILA

<sup>b)</sup>This alcohol dehydrogenase was cloned from *Thermoanaerobacter brockii* (Protein accession no: WP\_041589967.1).

## References :

[1] E. Vazquez-Figueroa, J. Chaparro-Riggers, A. S. Bommarius, *ChemBioChem* **2007**, *8*, 2295-2301.

## The primers used in this study

**Table S2.** The primers used for error-prone PCR

Primers	Sequences (5' to 3') <sup>a</sup>	Restriction sites
<i>PpGluDH-F-BamHI</i>	CGCGGATCCATGTCTACCATGATCGAATCTG	<i>BamHI</i>
<i>PpGluDH-R-HindIII</i>	CCCA <u>AAGCTT</u> TCAGACCACGCCCTGAGCCA	<i>HindIII</i>

<sup>a</sup>the restriction site is underlined.

**Table S3.** The primers used for saturation mutagenesis libraries construction

Category	Primers	Sequence (5' to 3') <sup>a</sup>
Mutation-R	K402X-F	TGGACAGC <u>NNK</u> CTGCACAACATCATGCAGTC
	I406X-F	TGCACAAC <u>NNK</u> ATGCAGTCGATTCACCATGC
	I410X-F	TGCAGTCG <u>NNK</u> CACCATGCATGCGTGCCTA
	A379X/L383X-F	GGCGT <u>ANDT</u> GTGTGGG <u>CNDT</u> GAAATGTGCGAGAACGCCAT
	T121X/L123X-F	TCGCTG <u>NDTT</u> CG <u>NDT</u> CCCATGGGCGGGCAAGGG
Mutation-R	K402X-R	TTGTGCAG <u>MNN</u> GCTGTCCACTTCAACGGCCG
	I406X-R	GACTGCAT <u>MNN</u> GTTGTGCAGCTTGCTGTCCA
	I410X-R	GCATGGT <u>MNN</u> CGACTGCATGATGTTGTGCA
	A379X/L383X-R	CATTCA <u>HN</u> GCCCGACACA <u>HN</u> TACGCCGCCCGCATTGGAGG
	T121X/L123X-R	CATGGGA <u>HN</u> CGA <u>HN</u> CAGCGAGTTCTTGAACACCT
Aid primers	Aid-F	TGAGATCCGGCTGCTAACAAA
	Aid-R	TTTGTTAGCAGCCGATCTCA

<sup>a</sup> underlined codon encodes desired amino acid substitution

**Table S4.** The primers used for back mutation analysis

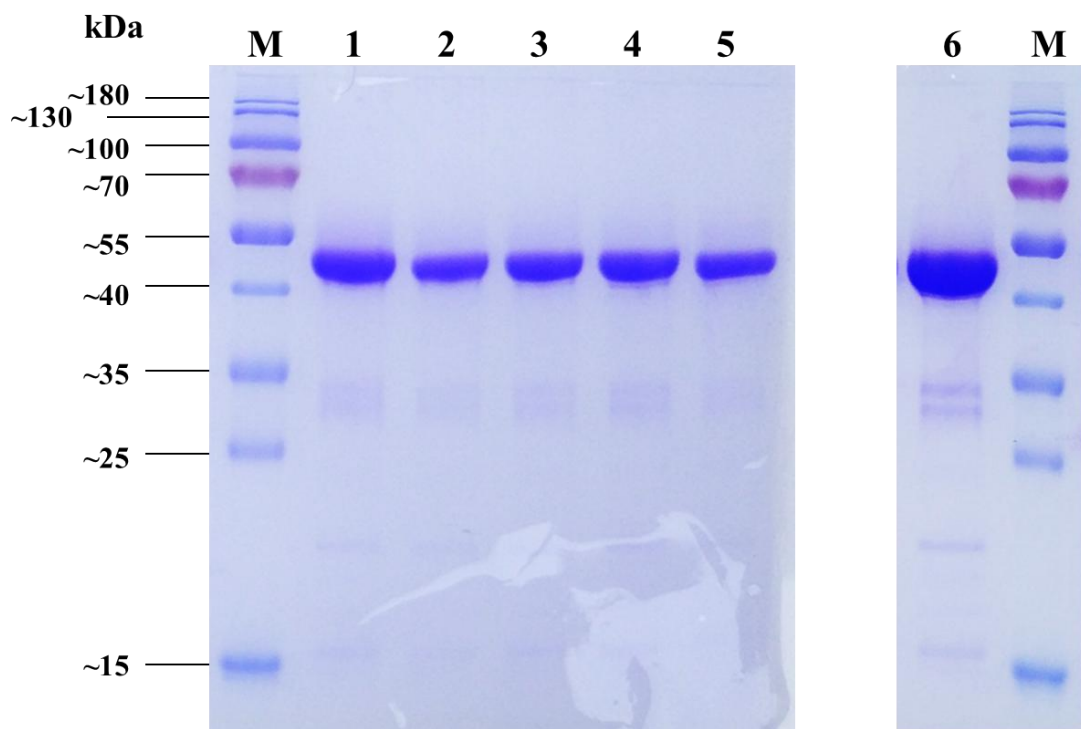
<b>Primers</b>	<b>Ssequences (5'to 3')a</b>	<b>Mutation (sites)</b>
<i>Pp</i> GluDH-V29A-F	ACCAGGCGGCAGAAAGAGGTGCTGCGCACCC	Val→Ala (29)
<i>Pp</i> GluDH-V29A-R	ACCTCTTCTGCCGCCTGGTGGAAATCCGGC	
<i>Pp</i> GluDH-M55V-F	TCGAGCGCGTTTGTGAGCCCCGAGCGCGCCG	Met→Val (55)
<i>Pp</i> GluDH-M55V-R	GGCTCGACAACGCGCTCGAGGATGCCGGAC	
<i>Pp</i> GluDH-K74M-F	ACCAGGGCATGGTGCAGGTCAACCGCGGCT	Lys→Met (74)
<i>Pp</i> GluDH-K74M-R	ACCTGCACCATGCCCTGGTCATCGACCCAA	
<i>Pp</i> GluDH-Q76R-F	GCAAGGTGCGTGTCAACCGCGGCTACCGCA	Gln→Arg (76)
<i>Pp</i> GluDH-Q76R-R	CGGTTGACACGCACCTTGCCCTGGTCATCG	
<i>Pp</i> GluDH-V102A-F	ACCCGTCGGCAAACCTCAGCGTGCTGAAGT	Val→Ala (102)
<i>Pp</i> GluDH-V102A-R	CTGAGGTTTGCCGACGGGTGGAAGCGCAGC	
<i>Pp</i> GluDH-F219Y-F	GCGTTTACTATGCCGAAGAAATGCTCAAGC	Phe→Tyr (219)
<i>Pp</i> GluDH-F219Y-R	TCTTCGGCATAGTAAACGCAGCCATAGCCG	
<i>Pp</i> GluDH-Y270H-F	GTACCTTGCATGCAGAAGCCGGGCTGACCG	Tyr→His (270)
<i>Pp</i> GluDH-Y270H-R	GCTTCTGCATGCAAGGTACCTTCAGAGTCA	
<i>Pp</i> GluDH-L354P-F	CGACTACCCCGGAGGCTGTGGATATCTTCC	Leu→Pro (354)
<i>Pp</i> GluDH-L354P-R	ACAGCCTCCGGGGTAGTCGGCATGTTGGCG	
<i>Pp</i> GluDH-I406T-F	TGCACAACACCATGCAGTCGATTACCATG	Ile→Thr (406)
<i>Pp</i> GluDH-I406T-R	GACTGCATGGTGTGTGCAGCTTGCTGTCC	
<i>Pp</i> GluDH-A379I-F	GCGGCGTAATTGTGTTCGGGCCTGGAAATGT	Ala→Ile (379)
<i>Pp</i> GluDH-A379I-R	CCCGACACAATTACGCCGCCCGCATTGGAG	
<i>Pp</i> GluDH-A379S-F	GCGGCGTAAGTGTGTTCGGGCCTGGAAATGT	Ala→Ser (379)
<i>Pp</i> GluDH-A379S-R	CCCGACACACTTACGCCGCCCGCATTGGAG	
<i>Pp</i> GluDH-A379V-F	GCGGCGTAGTTGTGTTCGGGCCTGGAAATGT	Ala→Val (379)
<i>Pp</i> GluDH-A379V-R	CCCGACACAACTACGCCGCCCGCATTGGAG	
<i>Pp</i> GluDH-A379F-F	GCGGCGTATTTGTGTTCGGGCCTGGAAATGT	Ala→Phe (379)
<i>Pp</i> GluDH-A379F-R	CCCGACACAATAACGCCGCCCGCATTGGAG	
<i>Pp</i> GluDH-A379Y-F	GCGGCGTATATGTGTTCGGGCCTGGAAATGT	Ala→Tyr (379)
<i>Pp</i> GluDH-A379Y-R	CCCGACACATATACGCCGCCCGCATTGGAG	
<i>Pp</i> GluDH-A379C-F	GCGGCGTATGTGTGTTCGGGCCTGGAAATGT	Ala→Cys (379)
<i>Pp</i> GluDH-A379C-R	CCCGACACACATACGCCGCCCGCATTGGAG	
<i>Pp</i> GluDH-L383Y-F	TGTCGGGCTATGAAATGTTCGCAGAACGCCA	Leu→Tyr (383)
<i>Pp</i> GluDH-L383Y-R	GACATTCATAGCCCGACACGGCTACGCCG	
<i>Pp</i> GluDH-L383C-F	TGTCGGGCTGTGAAATGTTCGCAGAACGCCA	Leu→Cys (383)
<i>Pp</i> GluDH-L383C-R	GACATTCACAGCCCGACACGGCTACGCCG	
<i>Pp</i> GluDH-L383S-F	TGTCGGGCAGTGAAATGTTCGCAGAACGCCA	Leu→Ser (383)
<i>Pp</i> GluDH-L383S-R	GACATTCACTGCCCGACACGGCTACGCCG	
<i>Pp</i> GluDH-T121S-F	GCGGCGTAATTGTGTTCGGGCCTGGAAATGT	Thr→Ser (121)
<i>Pp</i> GluDH-T121S-R	CCCGACACAATTACGCCGCCCGCATTGGAG	
<i>Pp</i> GluDH-T121N-F	ACTCGCTGTCTTCGCTGCCCATGGGCGGCG	Thr→Asn (121)
<i>Pp</i> GluDH-T121N-R	GGCAGCGAAGACAGCGAGTTCTTGAACACC	
<i>Pp</i> GluDH-T121V-F	ACTCGCTGGTTTCGCTGCCCATGGGCGGCG	Thr→Val (121)
<i>Pp</i> GluDH-T121V-R	GGCAGCGAAACCAGCGAGTTCTTGAACACC	

<i>Pp</i> GluDH-T121I-F	ACTCGCTG <u>ATT</u> TCGCTGCCCATGGGCGGCG	Thr→Ile (121)
<i>Pp</i> GluDH-T121I-R	GGCAGCGA <u>AA</u> TTCAGCGAGTTCTTGAACACC	
<i>Pp</i> GluDH-L123H-F	TGACCTCG <u>CA</u> TCCCATGGGCGGCGGCAAGG	Leu→His (123)
<i>Pp</i> GluDH-L123H-R	CCCATGGG <u>AT</u> GCGAGGTCAGCGAGTTCTTG	
<i>Pp</i> GluDH-L123Y-F	TGACCTCG <u>TAT</u> CCCATGGGCGGCGGCAAGG	Leu→Tyr (123)
<i>Pp</i> GluDH-L123Y-R	CCCATGGG <u>ATA</u> CGAGGTCAGCGAGTTCTTG	
<i>Pp</i> GluDH-L123S-F	TGACCTCG <u>AGT</u> CCCATGGGCGGCGGCAAGG	Leu→Ser (123)
<i>Pp</i> GluDH-L123S-R	CCCATGGG <u>ACT</u> CGAGGTCAGCGAGTTCTTG	
<i>Pp</i> GluDH-L123F-F	TGACCTCG <u>TTT</u> CCCATGGGCGGCGGCAAGG	Leu→Phe (123)
<i>Pp</i> GluDH-L123F-R	CCCATGGG <u>AA</u> ACGAGGTCAGCGAGTTCTTG	

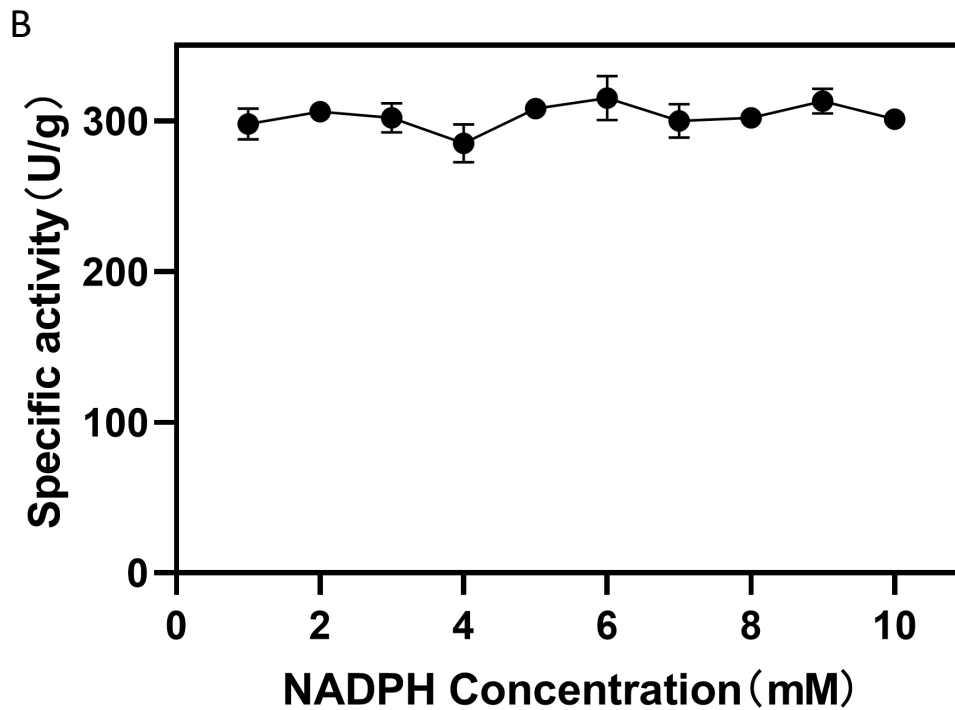
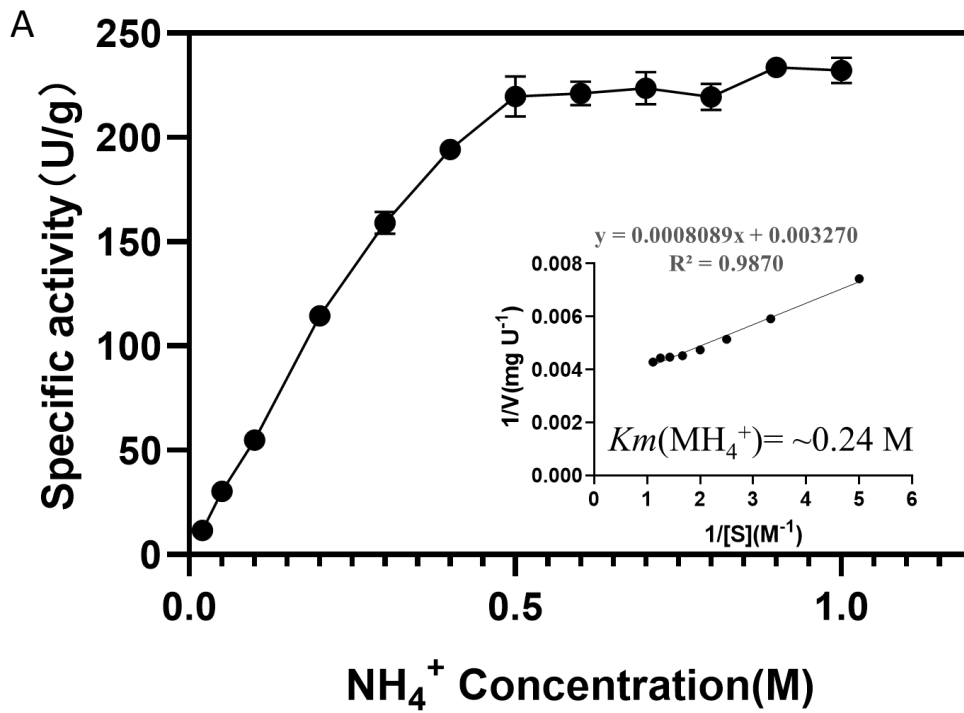
---

<sup>a</sup> underlined codon encodes desired amino acid substitution

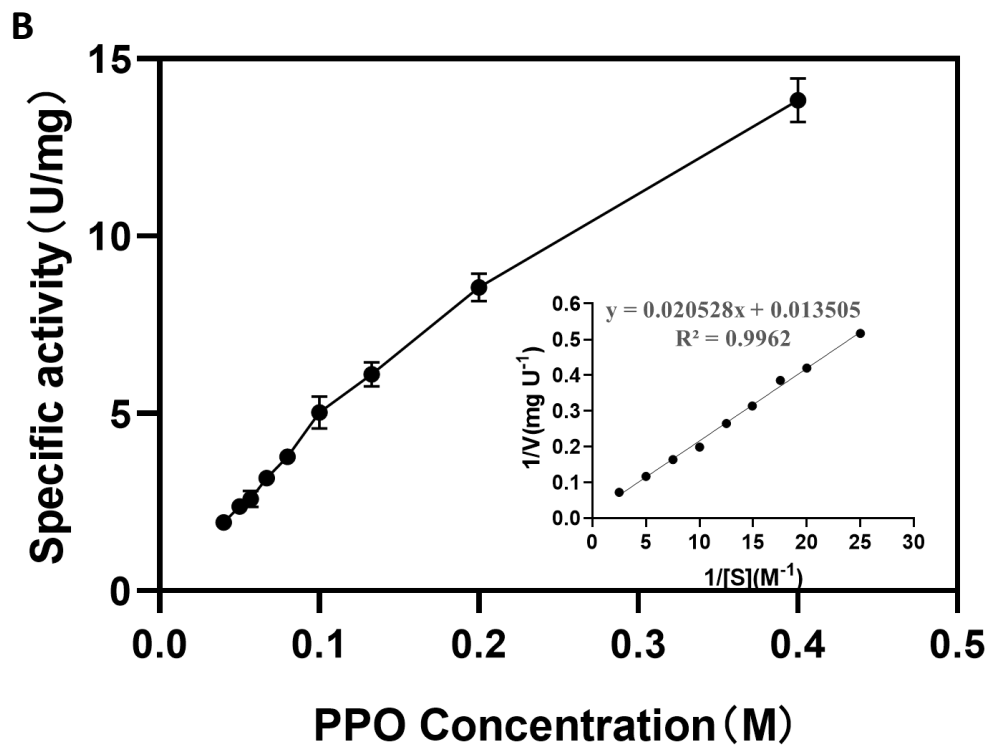
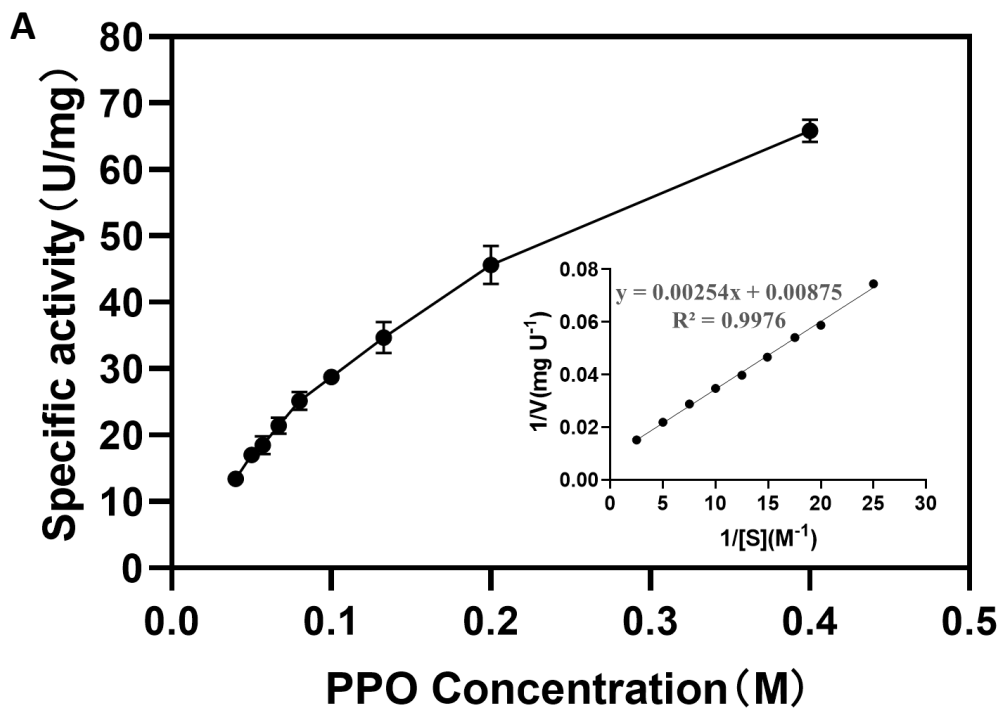




**Figure S12.** SDS-PAGE analysis of purified *PpGluDH* wild type (WT) and mutants. **Lane M** molecular weight marker, **Lane 1** purified wild type, **Lane 2** purified K402F, **Lane 3** purified I406F, **Lane 4** purified T121N/L123Y, **Lane 5** purified A379C/L383C, **Lane 6** purified A167G/A379S/L383Y.



**Figure S13.** Plots for the determination of  $\text{NH}_4^+$  and NADPH saturation values. (A)  $\text{NH}_4^+$ ; (B) NADPH.



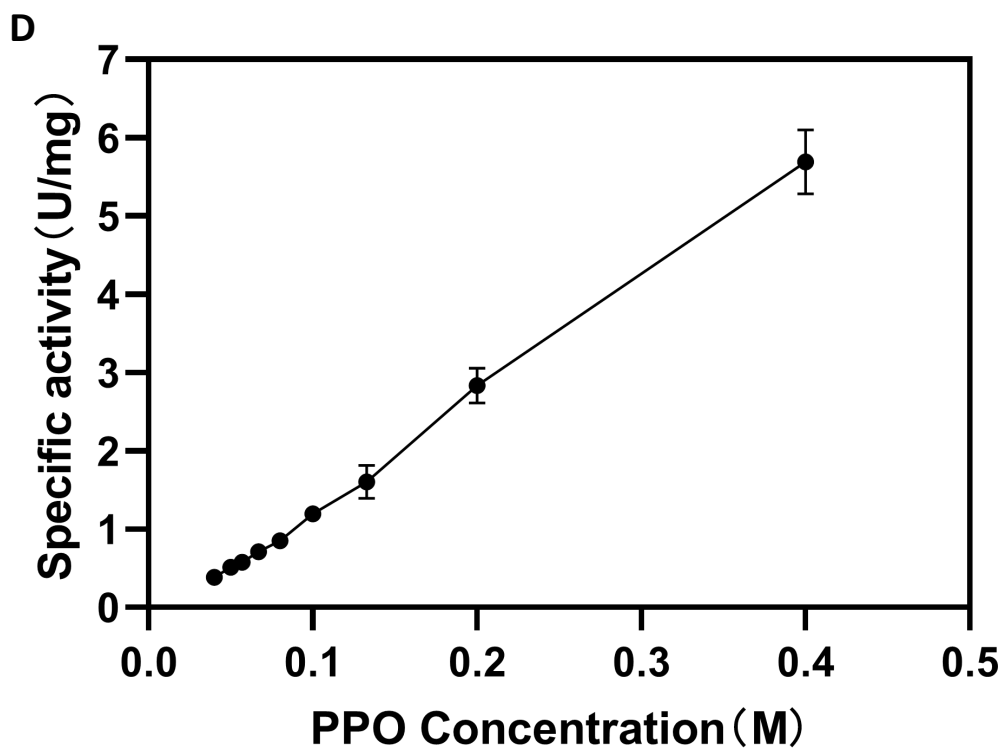
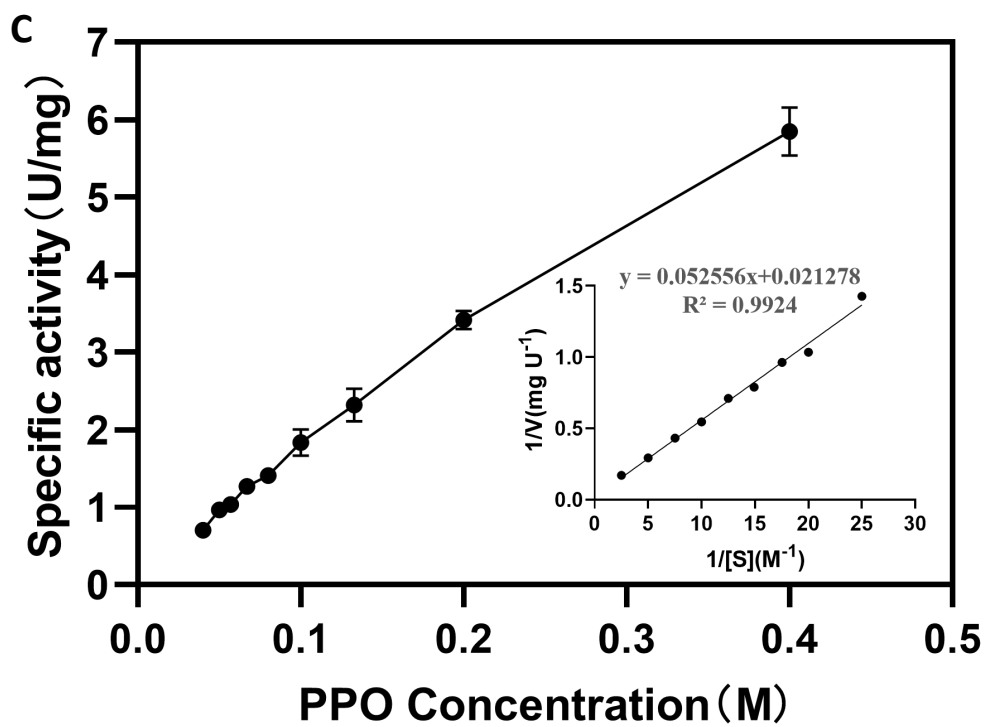


**Figure S14.** Michaelis-Menten plots for the kinetics of the hinge-engineered mutants with PPO. (A) T121N/L123Y; (B) A379C/L383C; (C) I406F; (D) K402F. Kinetic parameters of K402F can't be calculated because it's  $K_m$  is too high.

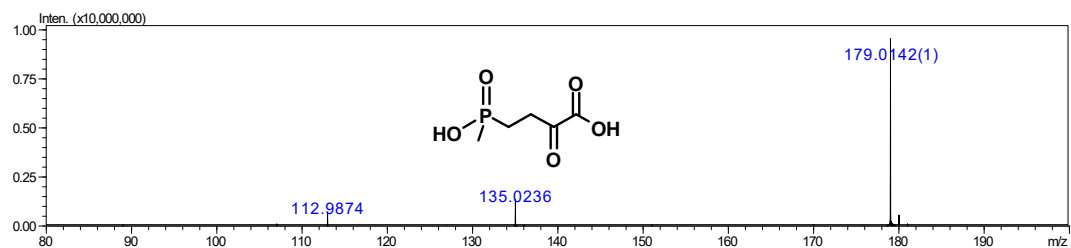


**Figure S15.** Mass spectrum (MS) of the synthesized substrate 2-oxo-4-[(hydroxy)(methyl)phosphinyl]butyric acid (PPO). IT-TOF (ESI):  $m/z=179.01$ , calcd. for  $C_5H_8O_5P$  [M]<sup>-</sup>: 179.01.

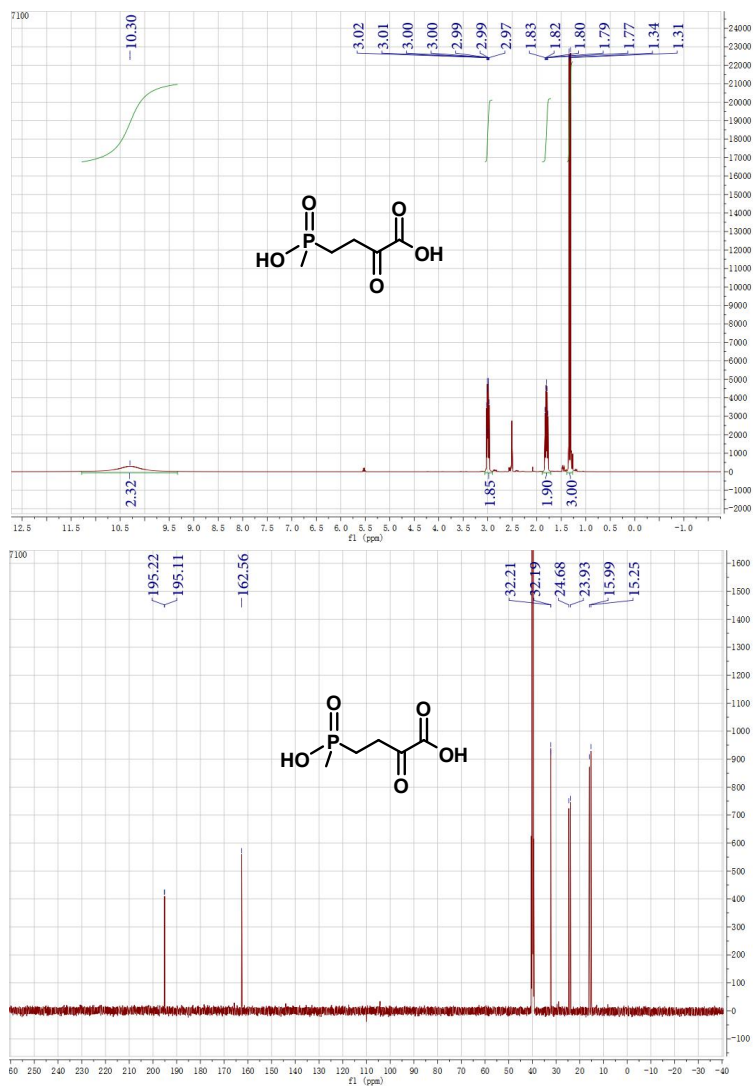


**Figure S16.** NMR spectra of the synthesized substrate 2-oxo-4-[(hydroxy)(methyl)phosphinyl]butyric acid (PPO). A.  $^1H$  NMR; B.  $^{13}C$  NMR.  $^1H$  NMR (500 MHz, DMSO)  $\delta$  10.30 (s, 2H), 3.06 – 2.91 (m, 2H), 1.89 – 1.71 (m, 2H), 1.33 (d,  $J$  = 14.1 Hz, 3H).  $^{13}C$  NMR (500 MHz, DMSO)  $\delta$  195.22, 195.11, 162.56, 32.21, 32.19, 24.68, 23.93, 15.99, 15.25.

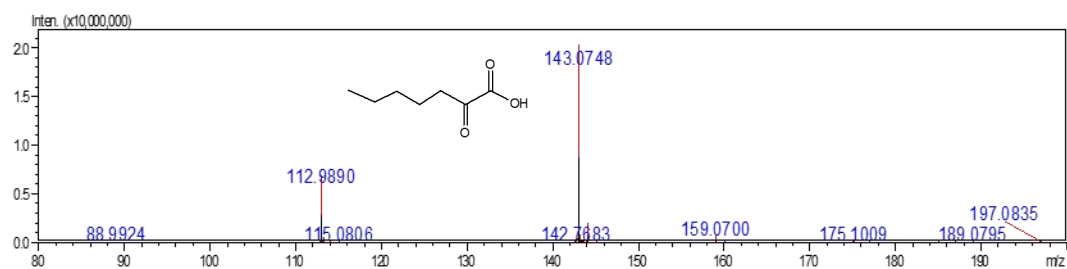


**Figure S17.** Mass spectrum (MS) of the synthesized substrate 2-oxoheptanoic acid (S8). IT-TOF (ESI):  $m/z=143.07$ , calcd. for  $C_7H_{11}O_3 [M]^-$ : 143.07.

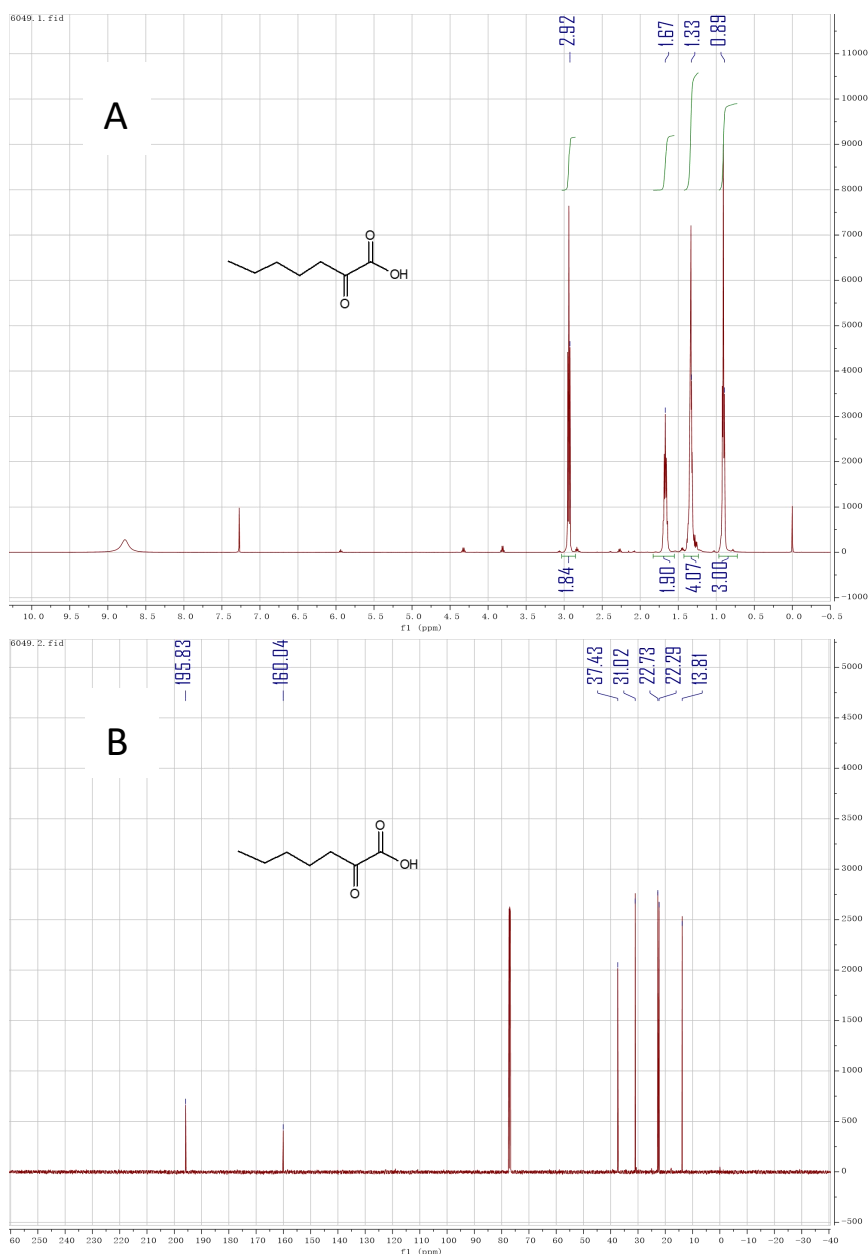


**Figure S18.** NMR spectra of the synthesized substrate 2-oxoheptanoic acid (S8). A.  $^1H$  NMR; B.  $^{13}C$  NMR.  $^1H$  NMR (500 MHz,  $CDCl_3$ )  $\delta$  2.94 (t,  $J=7.3$  Hz, 2H), 1.78 – 1.58 (m, 2H), 1.41 – 1.23 (m, 4H), 0.99 – 0.83 (m, 3H).  $^{13}C$  NMR (500 MHz,  $CDCl_3$ )  $\delta$  195.83, 160.04, 37.43, 31.02, 22.73, 22.29, 13.81.

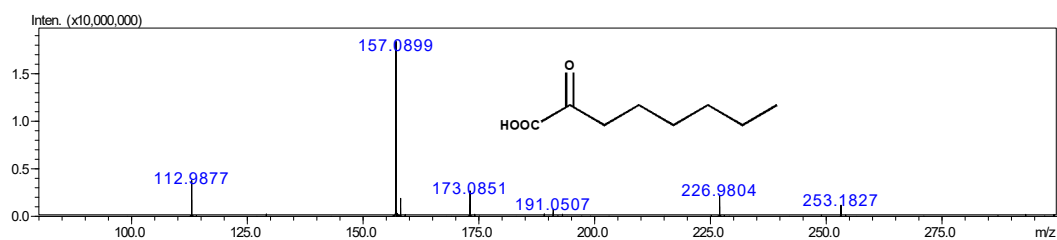


**Figure S19.** Mass spectrum (MS) of the synthesized substrate 2-oxooctanoic acid (S9). IT-TOF (ESI):  $m/z=157.09$ , calcd. for  $C_8H_{13}O_3 [M]^-$ : 157.09.

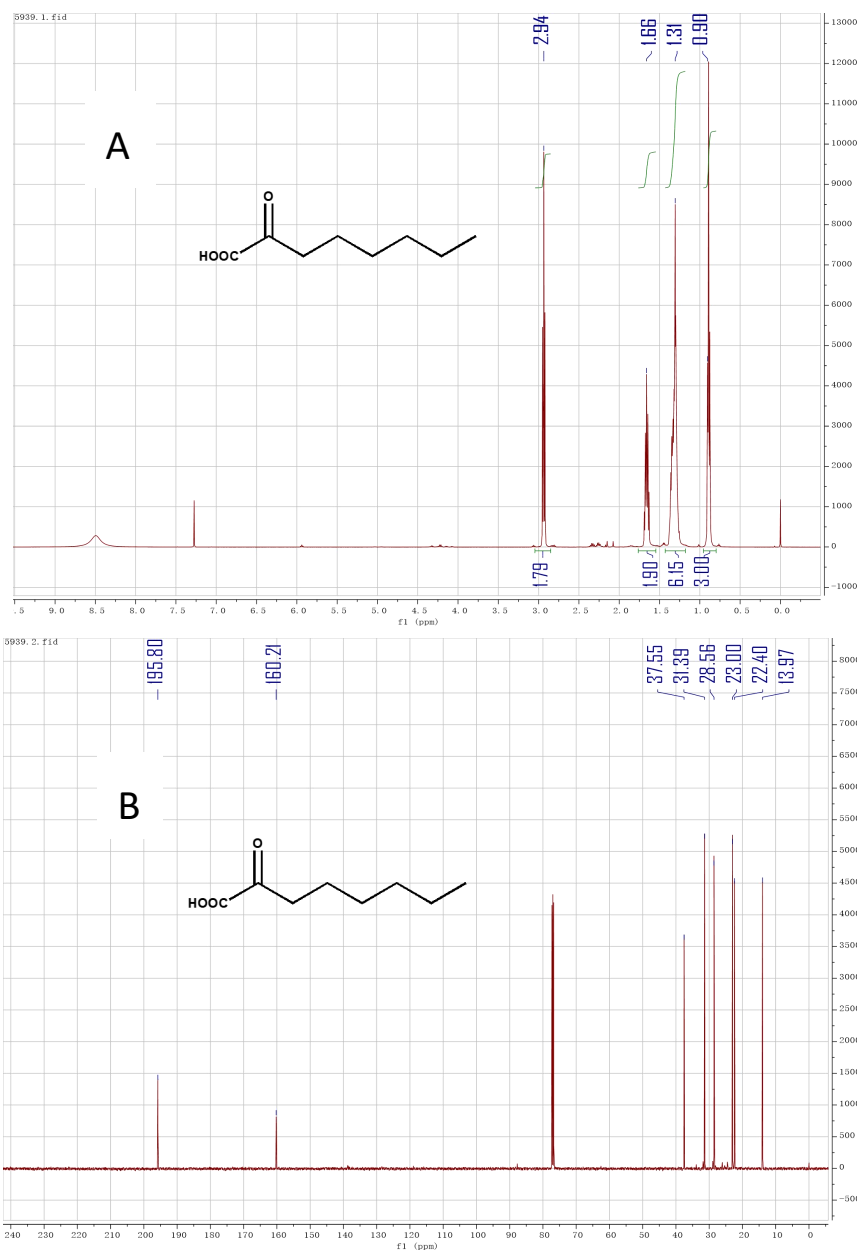


**Figure S20.** NMR spectra of the synthesized substrate 2-oxooctanoic acid (S9). A.  $^1H$  NMR; B.  $^{13}C$  NMR.  $^1H$  NMR (500 MHz,  $CDCl_3$ )  $\delta$  2.94 (t,  $J = 7.3$  Hz, 2H), 1.72 – 1.56 (m, 2H), 1.41 – 1.20 (m, 6H), 0.89 (t,  $J = 6.8$  Hz, 3H).  $^{13}C$  NMR (500 MHz,  $CDCl_3$ )  $\delta$  195.80, 160.21, 37.55, 31.39, 28.56, 23.00, 22.40, 13.97.

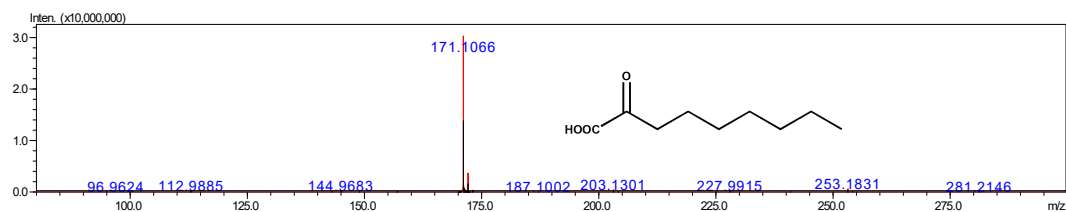


**Figure S21.** Mass spectrum (MS) of the synthesized substrate 2-oxononanoic acid (S10). IT-TOF (ESI):  $m/z=171.11$ , calcd. for  $C_9H_{15}O_3 [M]^-$ : 171.10.

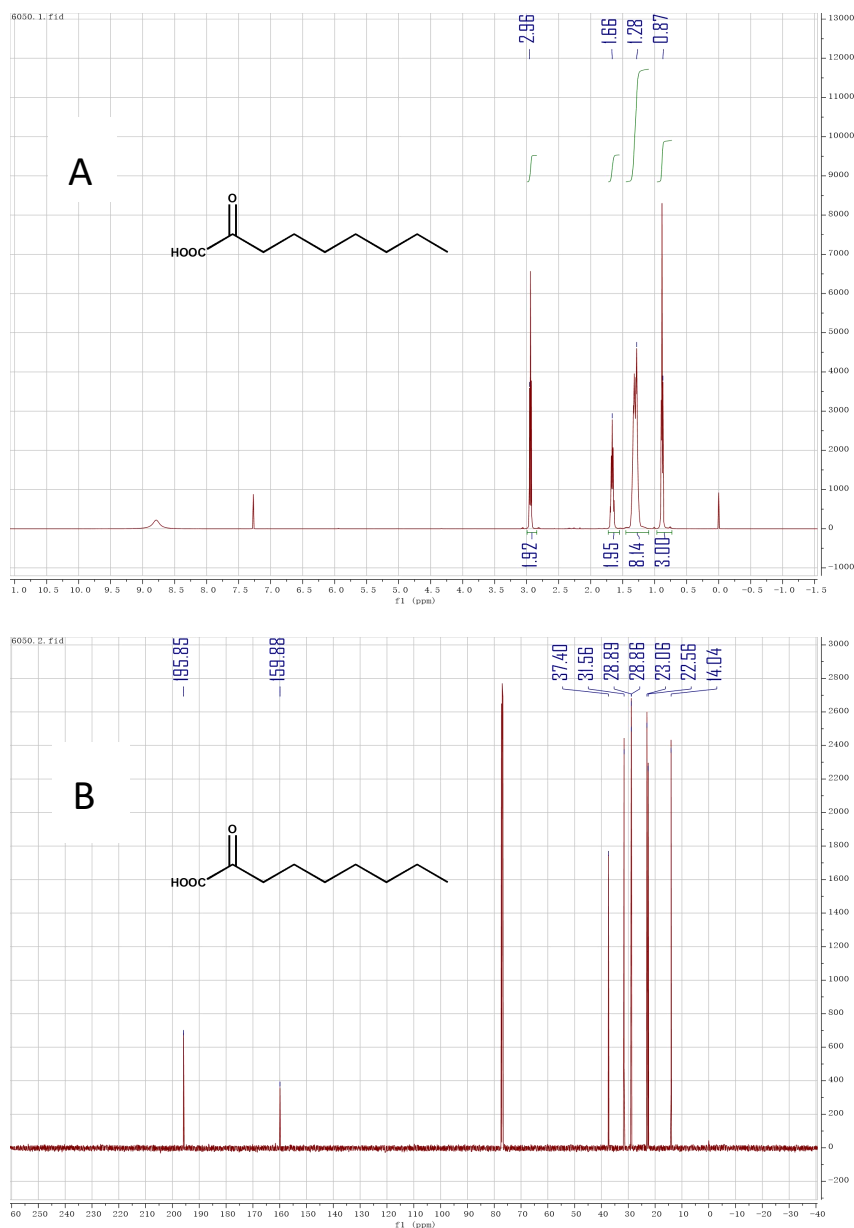


**Figure S22.** NMR spectra of the synthesized substrate 2-oxononanoic acid (S10). A.  $^1H$  NMR; B.  $^{13}C$  NMR.  $^1H$  NMR (500 MHz,  $CDCl_3$ )  $\delta$  2.94 (t,  $J = 7.3$  Hz, 2H), 1.74 – 1.54 (m, 2H), 1.42 – 1.20 (m, 8H), 0.88 (t,  $J = 6.9$  Hz, 3H).  $^{13}C$  NMR (500 MHz,  $CDCl_3$ )  $\delta$  195.85, 159.88, 37.40, 31.56, 28.89, 28.86, 23.06, 22.56, 14.04.



## **Purification process of the formed L-amino acids**

### **1) L-Phosphinothricin purification**

- a) When the PPO was almost exhausted, the reaction broth was heated to 75°C for 30 min;
- b) Denatured enzyme protein was removed by centrifugation and filtration;
- c) The ammonium ion was removed using an H-type weak cation exchange resin (D113);
- d) The resulting mixture was adjusted to pH 1.5 using hydrochloric acid;
- e) L-phosphinothricin was separated from the mixture using an H-type strong cation exchange resin (JK006) and eluted with ammonia;
- f) The L-phosphinothricin-containing fractions were adjusted to pH 2.5 and concentrated under reduced pressure;
- g) The L-phosphinothricin was crystallized in methanol + water mixture;
- h) The crystal was collected and then dried under vacuum.

### **2) L-Homophenylalanine purification**

- a) At the end of the reaction, the reaction broth was adjusted to pH <1 using hydrochloric acid;
- b) The insoluble impurities were removed by filtration;
- c) The filtrate was then adjusted to pH 5.5 using NaOH;
- d) The precipitated L-homophenylalanine was collected by filtration;
- e) The filter cake was washed using ddH<sub>2</sub>O for three times and then dried under vacuum.

### **3) L-2-Aminobutyric acid purification**

The isolation and purification of L-2-aminobutyric acid were carried out using a protocol described previously.<sup>[2]</sup>

## **References :**

[2] Tao, R.; Jiang, Y.; Zhu, F.; Yang, S., *Biotechnology Letters* 2014, 36 (4), 835-841.

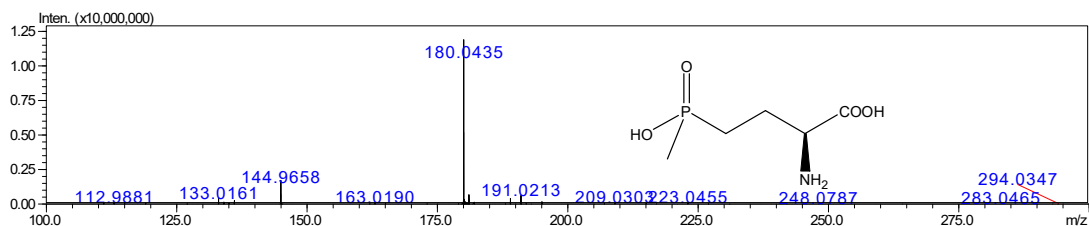


**Figure S23.** Mass spectrum (MS) of the purified L-phosphinothricin. IT-TOF (ESI):  $m/z=180.04$ , calcd. for  $C_5H_{11}NO_4P^- [M]$ : 180.14.

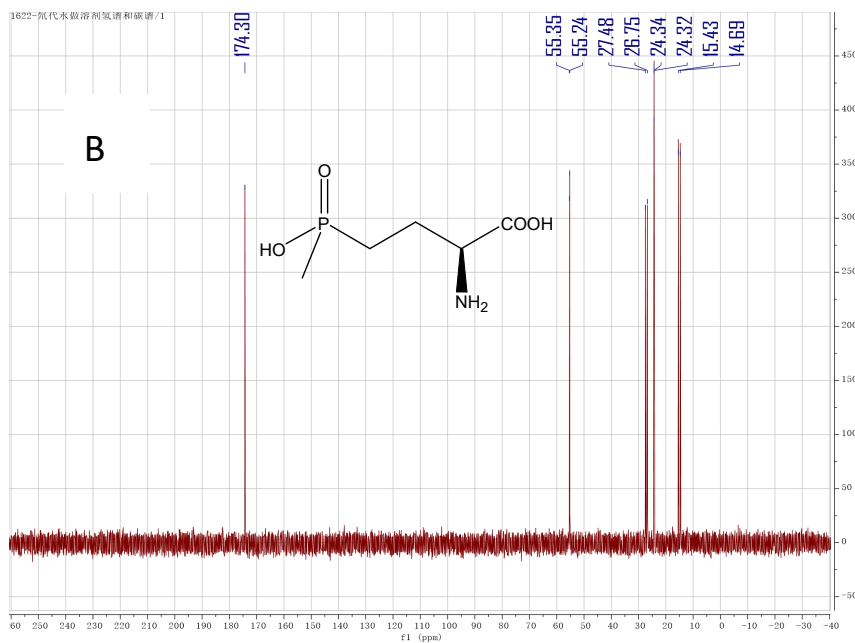
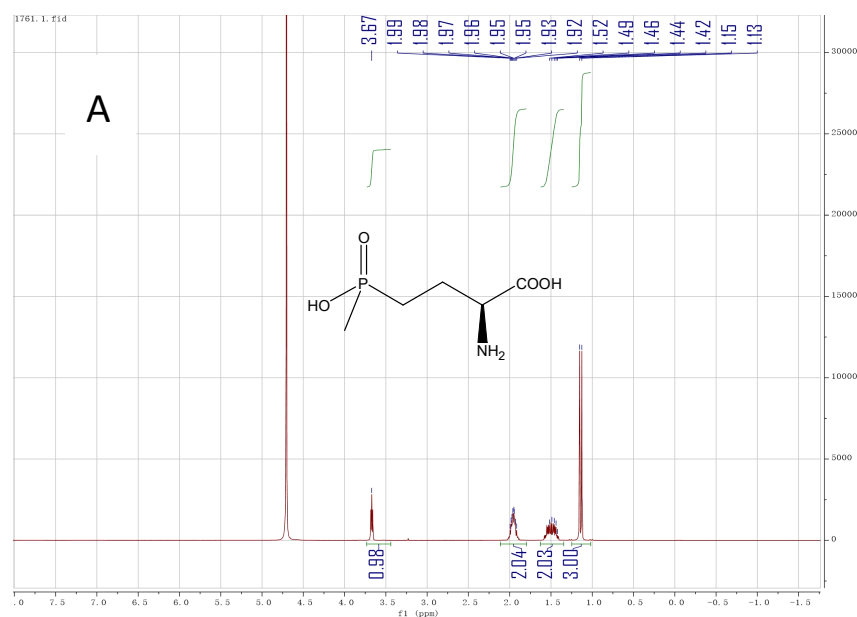


**Figure S24.** NMR spectra of the purified L-phosphinothricin. A.  $^1H$  NMR; B.  $^{13}C$  NMR.  $^1H$  NMR ( $^1H$  NMR (500 MHz,  $D_2O$ )  $\delta$  4.45 (s, 3H), 3.35 (t,  $J = 5.9$  Hz, 1H), 1.61 – 1.45 (m, 2H), 0.62 (t,  $J = 7.5$  Hz, 3H)..  $^{13}C$  NMR (500 MHz,  $D_2O$ )  $\delta$  174.30 , 55.29, 27.12, 24.33, 15.06.

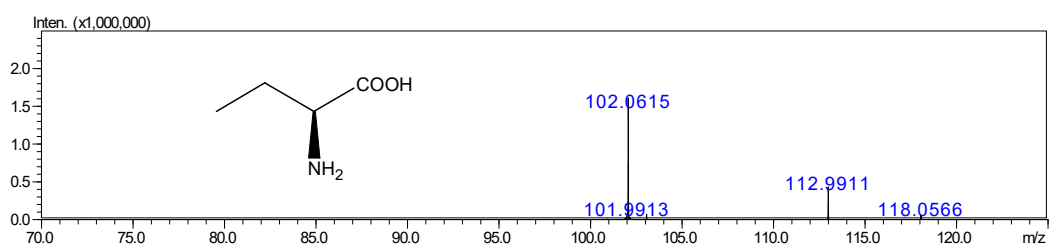


**Figure S25.** Mass spectrum (MS) of the purified L-2-aminobutyric acid. IT-TOF (ESI):  $m/z=102.06$ , calcd. for  $C_4H_9NO_2$  [M]<sup>-</sup>: 102.06.

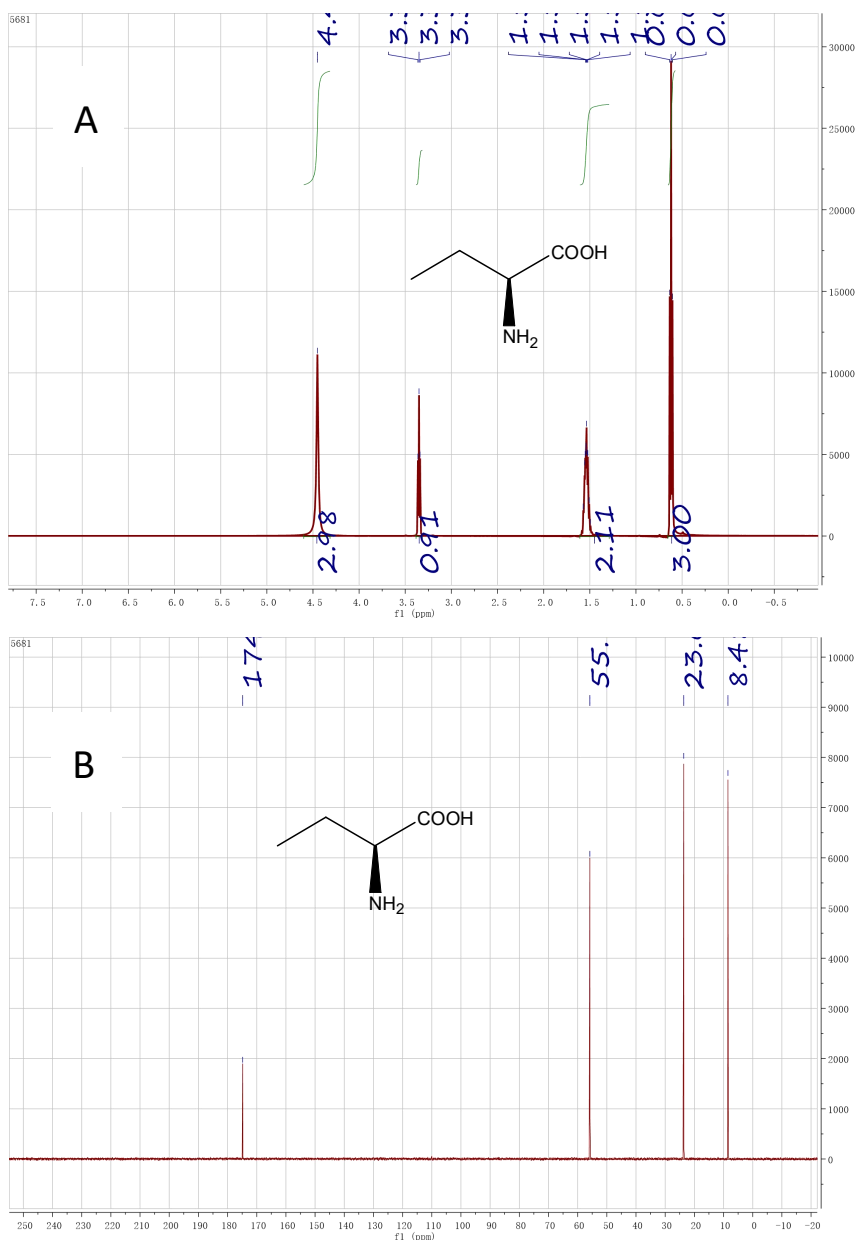


**Figure S26.** NMR spectra of the purified L-2-aminobutyric acid. A. <sup>1</sup>H NMR; B. <sup>13</sup>C NMR. <sup>1</sup>H NMR (500 MHz, D<sub>2</sub>O)  $\delta$  4.45 (s, 3H), 3.35 (t,  $J = 5.9$  Hz, 1H), 1.61 – 1.29 (m, 2H), 0.62 (t,  $J = 7.5$  Hz, 3H). <sup>13</sup>C NMR (500 MHz, D<sub>2</sub>O)  $\delta$  174.83, 55.81, 23.65, 8.48.

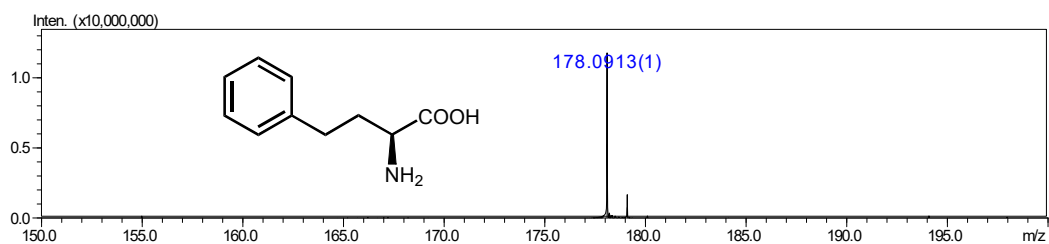


**Figure S27.** Mass spectrum (MS) of the purified L-homophenylalanine. IT-TOF (ESI):  $m/z=178.09$ , calcd. for  $C_{10}H_{13}NO_2$  [M]<sup>+</sup>: 108.09.

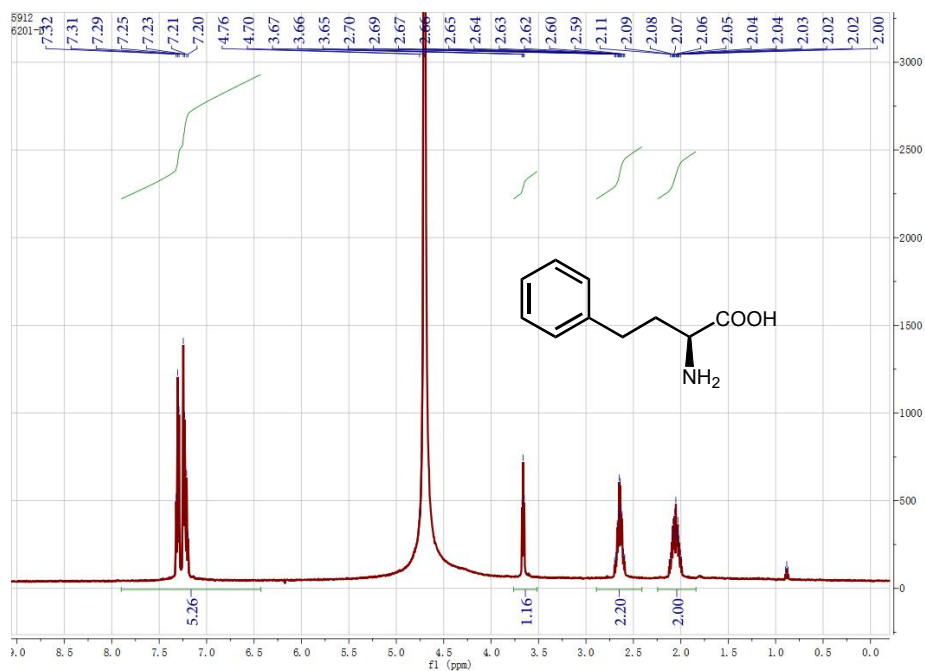


**Figure S28.** NMR spectrum of the purified L-homophenylalanine. <sup>1</sup>H NMR (500 MHz, D<sub>2</sub>O)  $\delta$  7.90 – 6.43 (m, 5H), 3.66 (t,  $J = 6.0$  Hz, 1H), 2.89 – 2.41 (m, 2H), 2.24 – 1.84 (m, 2H).